

Dirac formulation for universal quantum gates and Shor's integer factorization in high-frequency electric circuits

Motohiko Ezawa

Department of Applied Physics, University of Tokyo, Hongo 7-3-1, 113-8656, Japan

Quantum computation may well be performed with the use of electric circuits. Especially, the Schrödinger equation can be simulated by the lumped-element model of transmission lines, which is applicable to low-frequency electric circuits. In this paper, we show that the Dirac equation is simulated by the distributed-element model, which is applicable to high-frequency electric circuits. Then, a set of universal quantum gates (the Hadamard, phase-shift and CNOT gates) are constructed by networks made of transmission lines. We demonstrate Shor's prime factorization based on electric circuits. It will be possible to simulate any quantum algorithms simply by designing networks of metallic wires.

I. INTRODUCTION

Quantum computation is one of the hottest topic in physics^{1,2}. Various proposals have been made based on superconducting qubits³, ion trap⁴, photonic system⁵, quantum dots⁶ and nuclear magnetic resonance^{7,8}. For universal computations, it is enough to construct only three unitary gates, the Hadamard, phase-shift and CNOT gates, where all of the unitary gates are constructed by their combination⁹⁻¹¹. For instance, a set of universal quantum gates has been constructed based on quantum walk¹²⁻²¹. Shor's prime factorization²²⁻²⁴ has been demonstrated by using nuclear magnetic resonance^{7,25}, photonic systems²⁶⁻²⁹ and a Josephson junction³⁰.

Recently, it was shown that the Schrödinger equation is simulated by the lumped-element model of transmission lines³¹. Especially, a set of universal quantum gate has been constructed solely with the use of LC circuits³². This lumped-element model is only valid for low-frequency electric circuits. It corresponds to the tight-binding model in the context of condensed matter physics. On the other hand, the distributed-element model is appropriate for high-frequency electric circuits. It corresponds to the continuum theory.

In this paper, first we show that the transmission line is described by the one-dimensional Dirac equation, where the voltage and the current form a two-component wave function. Next, we construct a set of universal quantum gates consisting of the Hadamard, phase-shift and CNOT gates. Based on these gates, we make a demonstration of Shor's prime factorization. Our results will open a way to simulate quantum algorithms based on distributed-element electric circuits.

II. TRANSMISSION LINE AND THE DIRAC EQUATION

The electrodynamics along a transmission line is governed by the telegrapher equation made of

$$L \frac{d}{dt} I(x, t) = - \frac{\partial}{\partial x} V(x, t), \quad (1)$$

$$C \frac{d}{dt} V(x, t) = - \frac{\partial}{\partial x} I(x, t). \quad (2)$$

The first equation is the Kirchhoff voltage law, describing the voltage drop by the self-inductive electromotive force. The

second equation is the Kirchhoff current law.

We consider a bilayer system made of an insulator placed upon a metal: See Fig.1. Metallic wires deposited on this insulator plane are described by the telegrapher equations (1) and (2) with

$$C = \frac{2\pi\epsilon}{\log[2h/r]} [\text{F/m}], \quad (3)$$

$$L = \frac{\mu}{2\pi} \log \frac{2h}{r} [\text{H/m}], \quad (4)$$

where r is the radius of the metallic wire, and h is the distance between the wire and the metallic plane. The capacitive effect between the wire and the metallic plane leads to the capacitance C , while the origin of the inductance L is the self-inductive electromotive force.

The set of equations (1) and (2) are reformulated in the form of the one-dimensional Dirac equation,

$$i\partial_t \psi(x, t) = \mathcal{H} \psi(x, t), \quad (5)$$

with the wave function

$$\psi(x, t) = \begin{pmatrix} ZI(x, t) \\ V(x, t) \end{pmatrix}, \quad (6)$$

where $Z = \sqrt{L/C}$ is the characteristic impedance of the wire. The Hamiltonian is given by

$$\mathcal{H} = - \begin{pmatrix} 0 & \frac{i}{\sqrt{LC}} \frac{\partial}{\partial x} \\ \frac{i}{\sqrt{LC}} \frac{\partial}{\partial x} & 0 \end{pmatrix} = - \frac{i}{\sqrt{LC}} \sigma_x \frac{\partial}{\partial x}. \quad (7)$$

In the momentum space, it is reduced to

$$\mathcal{H} = \frac{1}{\sqrt{LC}} \sigma_x k, \quad (8)$$

whose eigenvalue is given by

$$E = \pm \frac{1}{\sqrt{LC}} |k|, \quad (9)$$

where k is the momentum. Its solution is a plane wave

$$\psi(x, t) = c_l e^{i(\omega t - kx)} + c_r e^{i(\omega t + kx)}, \quad (10)$$

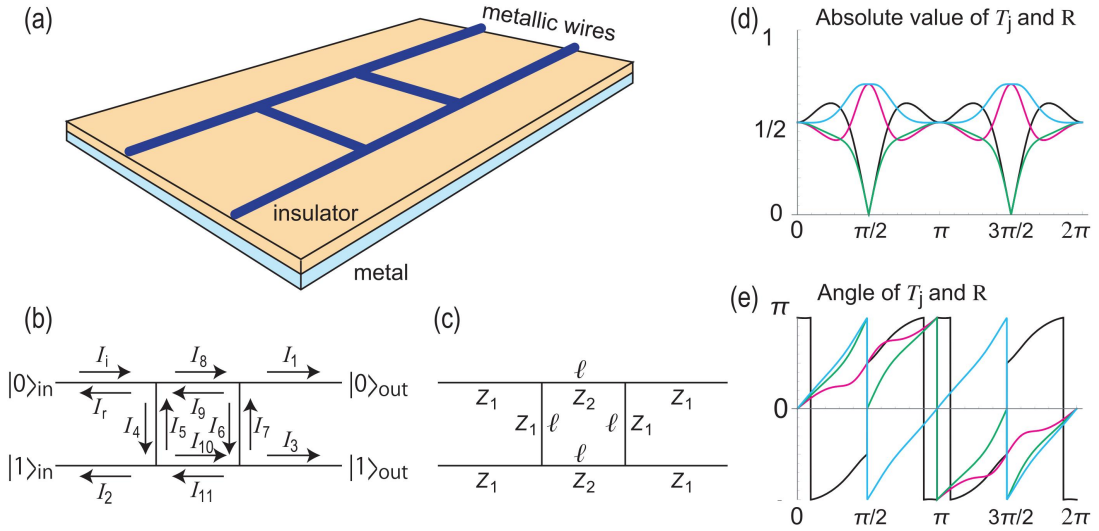


FIG. 1: (a) Illustration of a bilayer system made of a metallic plane and an insulator plane, upon which metallic wires are placed. This figure is for a mixing gate. (b) and (c) Current I_i and impedance Z_i with the index i are used in Appendix B. (d) and (e) The k dependence of the absolute value and the phase of the transmission coefficients $T_1(k)$, $T_2(k)$, $T_3(k)$ and the reflection coefficient $R(k)$. T_1 is colored in red, T_2 is colored in green, T_3 is colored in cyan and R is colored in black. The horizontal axis is the momentum $0 \leq k \leq 2\pi$. It is observed that $T_2(k) = R(k) = 0$ at $k\ell = \pi/2$ and $3\pi/2$. We have set $Z_2/Z_1 = 1/\sqrt{2}$.

where coefficients c_i and c_r are to be determined by the boundary conditions. Here the indices "i" and "r" stand for "injected" and "reflected", respectively.

The total energy $U_T = U_E + U_M$ is conserved along the transmission line, where

$$U_E = \frac{C}{2} \sum V^2, \quad U_M = \frac{L}{2} \sum I^2 \quad (11)$$

are the electrostatic energy and the magnetic energy, respectively. On the other hand, the probability of the wave function is rewritten in the form

$$\sum |\psi|^2 = \sum \mathcal{I}^2 + \mathcal{V}^2 = \sum \frac{L}{C} I^2 + V^2 = \frac{2}{C} U_T. \quad (12)$$

Hence, the conservation of the probability of the wave function is assured by the conservation of the total energy. This holds for a generic network made of several transmission lines.

III. QUANTUM GATES

One-qubit gates. A one-qubit gate U from the input $(|0\rangle_{\text{in}}, |1\rangle_{\text{in}})$ to the output $(|0\rangle_{\text{out}}, |1\rangle_{\text{out}})$ is defined by

$$\begin{pmatrix} |0\rangle_{\text{out}} \\ |1\rangle_{\text{out}} \end{pmatrix} = U \begin{pmatrix} |0\rangle_{\text{in}} \\ |1\rangle_{\text{in}} \end{pmatrix}. \quad (13)$$

In order to realize them, we use a two-port network of electric circuits with two inputs and two output as in Fig.1.

Linear electric circuits satisfy the superposition principle. We calculate the transmission and reflection coefficients when we input a plane wave only to the wire $|0\rangle_{\text{in}}$. There are three

other lines, where two of them are the outputs and the rest is the other input.

This is a scattering problem, and the wave functions are written in the form of

$$\langle x, 0 | \psi \rangle = e^{-ikx} + R(k) e^{ikx}, \quad (14)$$

$$\langle x, j | \psi \rangle = T_j(k) e^{ikx}, \quad j = 1, 2, 3. \quad (15)$$

In general, there is a reflection to the input. It is necessary to tune the parameters so as to cancel the reflection exactly, which we refer to as the no-reflection condition.

Mixing gate. As the first example of one-qubit gate, we study a double bridge structure shown in Fig.1, where two inputs and two output wires are attached to a square with length ℓ . The current-voltage relation is $V_i = Z_i I_i$, with Z_i being the characteristic impedance of the wire. The no-reflection condition is given by

$$I_r = I_2 = 0. \quad (16)$$

This condition leads to the impedance-matching relation

$$Z_2/Z_1 = 1/\sqrt{2}, \quad (17)$$

and the condition on the length ℓ

$$k\ell = \pi/2 \quad \text{or} \quad 3\pi/2, \quad (18)$$

as we derive in Appendix B: See (B.13) and (B.14). We show the transmission and reflection coefficients as a function of k and in Fig.1(d) and (e). It is observed that $T_2(k) = R(k) = 0$ at $k\ell = \pi/2$ and $k\ell = 3\pi/2$

Let us choose $k\ell = \pi/2$. Then, the transmission currents are obtained as

$$I_1/I_i = i/\sqrt{2}, \quad I_3/I_i = -1/\sqrt{2}. \quad (19)$$

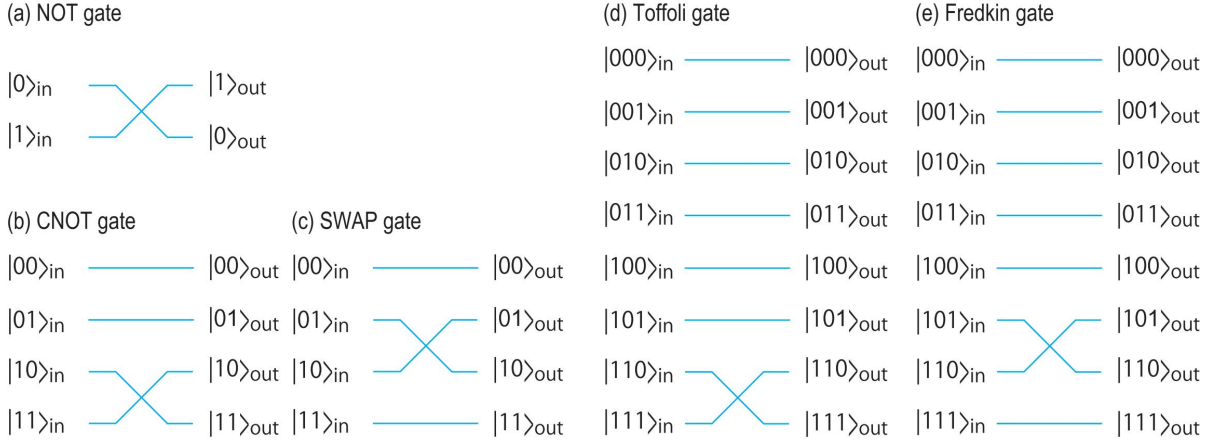


FIG. 2: Illustration of classical gates, where some wires are interchanged. (a) X (NOT) gate, (b) CNOT gate, (c) SWAP gate, (d) Toffoli gate and (e) Fredkin gate.

We compare these with the definition of one-qubit gate (13) to find that

$$U_{\text{mix}} = \frac{1}{\sqrt{2}} \begin{pmatrix} i & -1 \\ -1 & i \end{pmatrix}, \quad (20)$$

which is the mixing gate.

Phase-shift gate. As the second example of one-qubit gate, we study a phase-shift gate defined by

$$U_{\phi} = \begin{pmatrix} 1 & 0 \\ 0 & e^{i\phi} \end{pmatrix}. \quad (21)$$

It follows from (10) that the phase shift is a function of the length of a wire. Indeed, when the length of upper (lower) wire is ℓ_1 (ℓ_2) in a two-port network without any interaction between two wires, the phase shift is given by $e^{ik\ell_1}$ ($e^{ik\ell_2}$). It acts as a quantum gate,

$$\begin{pmatrix} e^{ik\ell_1} & 0 \\ 0 & e^{ik\ell_2} \end{pmatrix} = e^{ik\ell_1} \begin{pmatrix} 1 & 0 \\ 0 & e^{ik(\ell_2 - \ell_1)} \end{pmatrix}. \quad (22)$$

A phase delay is found to occur for an elongated wire. Since the overall phase is meaningless, the phase shift is given by $\phi = k(\ell_2 - \ell_1)$ in (21). We can construct a phase-shift gate (21) with an arbitrary phase by tuning the length of the elongated wire continuously. This is a merit comparing with the previous result in the lumped-electric circuit³². By tuning $k(\ell_2 - \ell_1) = \pi$, we can construct a Pauli Z gate $e^{ik\ell_1}\sigma_Z$.

Hadamard gate. The Hadamard gate is defined by

$$U_H = \frac{1}{\sqrt{2}} \begin{pmatrix} 1 & 1 \\ 1 & -1 \end{pmatrix}. \quad (23)$$

It is constructed by the combination of the mixing gate and the $3\pi/2$ phase-shift gate as $U_H = -iU_{3\pi/2}U_{\text{mix}}U_{3\pi/2}$.

NOT gate. The NOT gate U_X is given by the Pauli σ_x matrix, whose network is illustrated in Fig.2(a). It is constructed by interchanging the labels of the $|0\rangle$ and $|1\rangle$, as shown in Fig.2(b).

Two-qubit gates. We proceed to consider the four-port network,

$$\begin{pmatrix} |00\rangle_{\text{out}} \\ |01\rangle_{\text{out}} \\ |10\rangle_{\text{out}} \\ |11\rangle_{\text{out}} \end{pmatrix} = U \begin{pmatrix} |00\rangle_{\text{in}} \\ |01\rangle_{\text{in}} \\ |10\rangle_{\text{in}} \\ |11\rangle_{\text{in}} \end{pmatrix}. \quad (24)$$

The most well-known one is the CNOT gate defined by

$$U_{\text{CNOT}} = \begin{pmatrix} I_2 & O_2 \\ O_2 & U_X \end{pmatrix}, \quad (25)$$

where I_2 is the two-dimensional identity matrix, O_2 is the two-dimensional null matrix, and $U_X = \sigma_x$ is the NOT gate. We interchange the wires^{12,32} for the states $|10\rangle$ and $|11\rangle$, while we keep the states $|00\rangle$ and $|01\rangle$ as shown in Fig.2(b). Let the length of the wires for $|00\rangle$ and $|01\rangle$ to be ℓ_1 , and that of the wires for $|10\rangle$ and $|11\rangle$ to be ℓ_2 . Although $\ell_2 \neq \ell_1$, it is possible to suppress a phase shift between these two types of wires by setting $k(\ell_2 - \ell_1) = 2\pi$.

We similarly construct the SWAP gate by exchanging the wires $|10\rangle$ and $|01\rangle$ as in Fig.2(c).

Three-qubit gates. It is straightforward to construct three-qubits gates including the Toffoli and Fredkin gates. We exchange wires between $|110\rangle$ and $|111\rangle$ in the Toffoli gate as in Fig.2(d), while we exchange wires between $|101\rangle$ and $|110\rangle$ in the Fredkin gate as in Fig.2(e).

IV. SHOR'S INTEGER FACTORIZATION

As a demonstration we show how to perform Shor's integer factorization in electric circuits. Shor's algorithm is composed of quantum and classical parts. The quantum part is a period-finding algorithm, which consists of the Hadamard gate, the modular exponentiation and the inverse quantum Fourier transformation (QFT) as shown in Fig.3. We simulate the quantum part in an electric circuit.

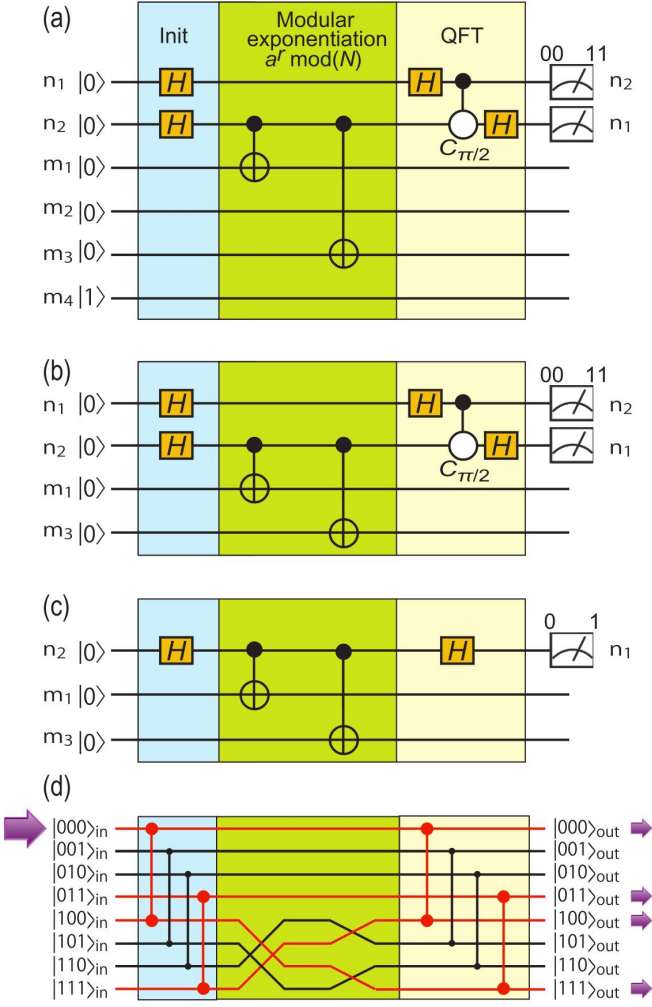


FIG. 3: (a) - (c) Quantum circuit^{26,30,33} for the period-finding routine of Shor's algorithm with $N = 15$ and $a = 11$. We note that n_1 and n_2 have been swapped in the output. Qubits m_2 and m_4 can be deleted since there is no action on these qubits, and (a) is simplified into (b). Since $U_H^2 = 1$, the qubit m_1 can be deleted, and (b) is simplified into (c). (d) Illustration of the corresponding electric circuit. The vertical line indicates the Hadamard gate. The current flows only in the red lines.

We study a typical example of the factorization of 15, whose quantum circuit^{26,29} is given in Fig.3(a). It consists of six qubits starting with the $|000001\rangle$, where the first two qubits (n_1, n_2) are called the register qubits while the last four qubits (m_1, m_2, m_3, m_4) are called the ancilla qubits. To simplify the calculation, we make a compilation of this quantum circuit^{26,29}. First, since there are no actions for the fourth and six qubits, they can be removed, and we obtain Fig.3(b). Next, the first qubit can be removed since we have $U_H^2 = 1$ and there is no action for the controlled phase-shift gate since the input is zero. By removing the first qubit, we have a compiled quantum circuit for three qubits shown in Fig.3(c). We implement it in the electric circuit as shown in Fig.3(d).

We start with a top most wire corresponding to $|000\rangle$. The output can be read out by measuring the magnitude and the

phase of the current for each wire. We would observe that the magnitudes of currents are identical for four wires $|000\rangle$, $|011\rangle$, $|100\rangle$ and $|111\rangle$ but the phase is different by 180 degree only for $|111\rangle$. Then the output is given by

$$\frac{1}{2} (|000\rangle + |011\rangle + |100\rangle - |111\rangle). \quad (26)$$

It is identical^{26,29} to the output for the quantum circuit for the period-finding routine of Shor's algorithm.

The result (26) is the one in the compiled circuit. By recovering the removed qubits, the output reads in the full quantum circuit as

$$\frac{1}{2} (|000001\rangle + |100001\rangle + |001011\rangle - |101011\rangle). \quad (27)$$

The compilation of (27) to (26) is understood by noting that the second qubit (0), the fourth qubit (0) and the sixth qubit (1) are common for all four terms in (27). Namely, since there is no action for the second, fourth and sixth qubits, there is no need to apply unitary transformation in the quantum circuit. Here we note that n_1 and n_2 have been swapped after the QFT¹¹. It follows from (27) that the register qubits are $|00\rangle$ and $|10\rangle$. As reviewed in Appendix C, we find the period $r = 2$ from this output, and we obtain the prime factorization $15 = 3 \times 5$.

V. CONCLUSION

We have constructed a set of universal quantum gates based on the distributed-element model applicable to high-frequency electric circuits. We can construct them only by using metallic wires deposited on an insulating layer placed on the metallic layer. The size of the system will be greatly reduced to the order of 10nm. Our results will open a way for integrated circuits for simulating quantum algorithms.

Acknowledgement

The author is very much grateful to A. Kurobe, E. Saito and N. Nagaosa for helpful discussions on the subject. This work is supported by the Grants-in-Aid for Scientific Research from MEXT KAKENHI (Grants No. JP17K05490 and No. JP18H03676). This work is also supported by CREST, JST (JPMJCR16F1).

Appendix A: Y-junction

We study a transmission through a Y-junction (Fig.4). There are three legs, which we call the leg- i . We inject a current I_i to the leg-1. There is a reflected current I_r by the junction in general. Thus, two currents flow on the leg-1, with the total current being $I_i - I_r$. Let Z_i be the characteristic impedance of the leg- i . The voltage V_i and the current I_i are related by the impedance Z_i as

$$V_i = Z_1 I_i, \quad V_r = Z_1 I_r, \quad V_2 = Z_2 I_2, \quad V_3 = Z_3 I_3. \quad (A.1)$$

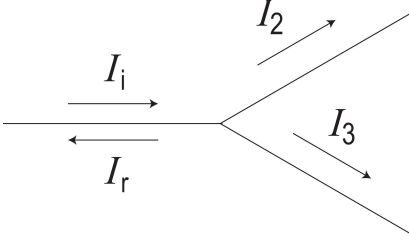


FIG. 4: (a) Illustration of the Y junction. The numbers i show the index for I_i .

At the junction, the current conservation gives

$$I_i - I_r = I_2 + I_3, \quad (\text{A.2})$$

while the voltages are related as

$$V_i + V_r = V_2 = V_3. \quad (\text{A.3})$$

It follows from (A.1), (A.3) and (A.2) that

$$V_r = \frac{Z_2 Z_3 - Z_1 (Z_2 + Z_3)}{Z_1 Z_2 + Z_2 Z_3 + Z_3 Z_1}, \quad (\text{A.4})$$

$$I_r = -\frac{Z_2 Z_3 - Z_1 (Z_2 + Z_3)}{Z_1 (Z_1 Z_2 + Z_2 Z_3 + Z_3 Z_1)}. \quad (\text{A.5})$$

We require no reflection at the junction, which implies

$$V_r = I_r = 0. \quad (\text{A.6})$$

Solving (A.4) and (A.5) with (A.6), we obtain

$$Z_1 = \frac{Z_2 Z_3}{Z_2 + Z_3}, \quad (\text{A.7})$$

which is the impedance matching condition. Consequently, we obtain

$$V_2 = Z_1 I_i, \quad V_3 = Z_1 I_i, \quad (\text{A.8})$$

$$I_2 = \frac{Z_3}{Z_2 + Z_3} I_i, \quad I_3 = \frac{Z_2}{Z_2 + Z_3} I_i \quad (\text{A.9})$$

for the transmissions along the leg-2 and the leg-3.

Appendix B: Mixing gate

We study a transmission through the mixing gate (Fig.1), where two inputs and two output wires are attached to a square with length ℓ . By using the notation for the currents in Fig.1(b), the current conservations give

$$I_i - I_r - I_4 + I_5 - I_8 + I_9 = 0, \quad (\text{B.1})$$

$$-I_2 + I_4 e^{ik\ell} - I_5 e^{-ik\ell} - I_{10} + I_{11} = 0, \quad (\text{B.2})$$

$$-I_1 - I_6 + I_7 + I_8 e^{ik\ell} - I_9 e^{-ik\ell} = 0, \quad (\text{B.3})$$

$$-I_3 + I_6 e^{ik\ell} - I_7 e^{-ik\ell} + I_{10} e^{ik\ell} - I_{11} e^{-ik\ell} = 0, \quad (\text{B.4})$$

while the voltage relations are

$$V_i + V_r = V_4 + V_5 = V_8 + V_9, \quad (\text{B.5})$$

$$V_1 = V_8 e^{ik\ell} + V_9 e^{-ik\ell} = V_6 + V_7, \quad (\text{B.6})$$

$$V_2 = V_4 e^{ik\ell} + V_5 e^{-ik\ell} = V_{10} + V_{11}, \quad (\text{B.7})$$

$$V_3 = V_6 e^{ik\ell} + V_7 e^{-ik\ell} = V_{10} e^{ik\ell} + V_{11} e^{-ik\ell}. \quad (\text{B.8})$$

The current-voltage relation reads

$$V_i = Z_i I_i, \quad (\text{B.9})$$

with Z_i being the characteristic impedance of the wire.

When we assume $Z_i = Z_1$ for $i = i, r, 1, \dots, 7$ and $Z_i = Z_2$ for $i = 8, \dots, 11$ as shown in Fig.1(c), we can solve these equations as

$$I_r/I_i = Z_1^2 \frac{2Z_2^2 - Z_1^2}{Z_1^4 + 4Z_2^4}, \quad I_2/I_i = 2iZ_2^2 \frac{2Z_2^2 - Z_1^2}{Z_1^4 + 4Z_2^4}, \quad (\text{B.10})$$

$$I_1/I_i = \frac{Z_1^3 Z_2}{Z_1^4 + 4Z_2^4}, \quad I_3/I_i = \frac{Z_1 Z_2^3}{Z_1^4 + 4Z_2^4}, \quad (\text{B.11})$$

for

$$k\ell = \pm\pi/2, \quad (\text{B.12})$$

which is (18) in the text. Imposing the no-reflection condition ($I_r = I_2 = 0$) on (B.10), we have the impedance matching condition

$$Z_2/Z_1 = 1/\sqrt{2}, \quad (\text{B.13})$$

which is (17) in the text. From (B.11) we obtain

$$I_1/I_i = \pm i/\sqrt{2}, \quad I_3/I_i = -1/\sqrt{2}. \quad (\text{B.14})$$

By comparing (B.14) with Fig.1(b), it is found to act as

$$U_{\text{mix}} = \frac{1}{\sqrt{2}} \begin{pmatrix} \pm i & -1 \\ -1 & \pm i \end{pmatrix}, \quad (\text{B.15})$$

which is the mixing gate (20) for $k\ell = \pi/2$ in the text.

Appendix C: Shor's algorithm

We review Shor's algorithm²²⁻²⁴ for prime factorization of an integer N with the aid of the period r . It consists of three steps. The first step is to design a modular exponentiation part of a quantum circuit, which is done by a classical computer. The second step to find the period r , which is done by a quantum computer. The final step is to obtain prime factors from r , which is done by a classical computer.

We factorize an integer $N = pq$, with both p and q being odd primes. We pick a random number a satisfying $0 < a < N$, which has no common factor with N . We define the modular exponential function by

$$f(x) = a^x \pmod{N}. \quad (\text{C.1})$$

The Euler theorem dictates that there is a positive integer r satisfying

$$f(r) = a^r \pmod{N} = 1. \quad (\text{C.2})$$

There is a periodicity,

$$f(x+r) = f(x), \quad (\text{C.3})$$

since

$$a^{x+r} \pmod{N} = a^r \pmod{N}. \quad (\text{C.4})$$

Then, we find

$$a^r - 1 = cN \quad (\text{C.5})$$

with an integer c . It is rewritten as

$$(a^{r/2} + 1)(a^{r/2} - 1) = cN. \quad (\text{C.6})$$

If r is an even number, at least one nontrivial factor of N is given by the greatest common denominator of $\gcd(a^{r/2} + 1, N)$ or $\gcd(a^{r/2} - 1, N)$. It is solved by using the Euclidean algorithm, which is efficiently calculated by a classical computer. If r is an odd number, we rechoose a different number a and redo the process.

Shor's algorithm provides us with an efficient quantum circuit to find the period r . We initialize the state as

$$\left(\bigotimes_n |0\rangle \right) \left(\bigotimes_{m-1} |0\rangle \right) \otimes |1\rangle, \quad (\text{C.7})$$

where the first n qubits are the register qubits while the second m qubits are the ancilla qubits. We choose m such that $2^{m-1} < N \leq 2^m$, and a certain integer n of the order of m .

We first apply the Hadamard gates on the register qubits, which transforms the initialized state as

$$\bigotimes_n |0\rangle \mapsto \frac{1}{\sqrt{2^n}} (|0\rangle + |1\rangle)^{\otimes n} = \frac{1}{\sqrt{2^n}} \sum_{x=0}^{2^n-1} |x\rangle, \quad (\text{C.8})$$

where $|x\rangle$ stands for the binary representation of x . By applying the modular exponentiation to the ancilla qubits, (C.7) leads to,

$$\frac{1}{\sqrt{2^n}} \sum_{x=0}^{2^n-1} |x\rangle |a^x \pmod{N}\rangle. \quad (\text{C.9})$$

Next, we apply a QFT to the register qubits, obtaining

$$\frac{1}{2^n} \sum_{y=0}^{2^n-1} \sum_{x=0}^{2^n-1} e^{2\pi i xy/2^n} |y\rangle |a^x \pmod{N}\rangle. \quad (\text{C.10})$$

We reorder this sum as

$$\frac{1}{2^n} \sum_{z=0}^{N-1} \sum_{y=0}^{2^n-1} \left[\sum_{x=\{0, \dots, 2^n-1\}; f(x)=z} e^{2\pi i xy/2^n} \right] |y\rangle |z\rangle. \quad (\text{C.11})$$

Since x is periodic as in (C.3), we can write it as

$$x = x_0 + rb, \quad (\text{C.12})$$

with b being an integer. The sum is calculated as

$$\begin{aligned} & \sum_{x=\{0, \dots, 2^n-1\}; f(x)=z} e^{2\pi i xy/2^n} \\ &= e^{2\pi i x_0 y/2^n} \sum_{b=0}^{m-1} e^{2\pi i rby/2^n}, \end{aligned} \quad (\text{C.13})$$

where

$$m-1 = \left\lfloor \frac{2^n - x_0 - 1}{r} \right\rfloor \quad (\text{C.14})$$

with the use of a floor function. The absolute value of the coefficient of the state $|y\rangle |z\rangle$ is given by

$$\left| \frac{1}{2^n} \sum_{b=0}^{m-1} e^{2\pi i rby/2^n} \right|, \quad (\text{C.15})$$

where

$$\frac{1}{2^n} \sum_{b=0}^{m-1} e^{2\pi i rby/2^n} = \begin{cases} 1 & \text{if } e^{2\pi i ry/2^n} = 1 \\ \frac{1}{2^n} \frac{e^{2\pi i rmy/2^n} - 1}{e^{2\pi i ry/2^n} - 1} & \text{if } e^{2\pi i ry/2^n} \neq 1 \end{cases}. \quad (\text{C.16})$$

Hence the coefficient of the register qubits $|y\rangle$ becomes negligible unless

$$ry/2^n \in \mathbb{Z}. \quad (\text{C.17})$$

Consequently, r can be determined. The prime factors are given by the nontrivial greatest common divisor of $a^{r/2} \pm 1$.

We take an example^{26,29} of $N = 15$. Let us choose $a = 11$. We use $m = 4$ for ancilla qubits to satisfy $2^{m-1} < 15 \leq 2^m$. It is enough to use $n = 2$ for the register qubits^{26,29}. Then, by calculating (C.9), we find

$$\begin{aligned} & \frac{1}{2} \sum_{x=0}^3 |x\rangle |11^x \pmod{15}\rangle \\ &= \frac{1}{2} (|0\rangle |1\rangle + |1\rangle |11\rangle + |2\rangle |1\rangle + |3\rangle |11\rangle) \\ &= \frac{1}{2} ((|0\rangle + |2\rangle) |1\rangle + (|1\rangle + |3\rangle) |11\rangle). \end{aligned} \quad (\text{C.18})$$

In the binary representation, it becomes

$$\frac{1}{2} (|00\rangle |0001\rangle + |01\rangle |1011\rangle + |10\rangle |0001\rangle + |11\rangle |1011\rangle). \quad (\text{C.19})$$

The inverse QFT with respect to the register qubits is explicitly given by

$$U_{\text{QFT2}}^{-1} = \frac{1}{2} \begin{pmatrix} 1 & 1 & 1 & 1 \\ 1 & -i & -1 & i \\ 1 & -1 & 1 & -1 \\ 1 & i & -1 & -i \end{pmatrix}. \quad (\text{C.20})$$

After the inverse QFT, (C.19) becomes

$$\begin{aligned}
& \frac{1}{4} (|00\rangle + |01\rangle + |10\rangle + |11\rangle) |0001\rangle \\
& + \frac{1}{4} (|00\rangle - i|01\rangle - |10\rangle + i|11\rangle) |1011\rangle \\
& + \frac{1}{4} (|00\rangle - |01\rangle + |10\rangle - |11\rangle) |0001\rangle \\
& + \frac{1}{4} (|00\rangle + i|01\rangle - |10\rangle - i|11\rangle) |1011\rangle \\
& = \frac{1}{2} (|00\rangle + |10\rangle) |0001\rangle + \frac{1}{2} (|00\rangle - |10\rangle) |1011\rangle \\
& = \frac{1}{2} (|000001\rangle + |100001\rangle + |001011\rangle - |101011\rangle).
\end{aligned} \tag{C.21}$$

We focus on the register qubits, where there are only two

states $|00\rangle$ and $|10\rangle$, or $|0\rangle$ and $|2\rangle$ in the decimal unit. They imply $y = 0$ and $y = 2$. By substituting $y = 2$ and $n = 2$ in (C.17), we find $r = 2$.

The prime factorization of $N = 15$ is done once we find the period $r = 2$ for the choice of $a = 11$. Then,

$$a^{r/2} + 1 = 12, \quad a^{r/2} - 1 = 10. \tag{C.22}$$

The greatest common divisor c is found from (C.6) as

$$c = (a^{r/2} + 1)(a^{r/2} - 1)/N = 8. \tag{C.23}$$

Using the Euclidian algorithm, we have

$$\gcd(12, 15) = 3, \quad \gcd(10, 15) = 5, \tag{C.24}$$

and hence that $15 = 3 \times 5$.

-
- ¹ R. Feynman, *Int. J. Theor. Phys.* 21, 467 (1982).
² D. P. DiVincenzo, *Science* 270, 255 (1995).
³ Y. Nakamura; Yu. A. Pashkin; J. S. Tsai, *Nature* 398, 786 (1999)
⁴ J. I. Cirac and P. Zoller, *Phys. Rev. Lett.* 74, 4091 (1995)
⁵ E. Knill, R. Laflamme and G. J. Milburn, *Nature*, 409, 46 (2001)
⁶ D. Loss and D. P. DiVincenzo, *Phys. Rev. A* 57, 120 (1998)
⁷ L. M.K. Vandersypen, M. Steffen, G. Breyta, C. S. Yannoni, M. H. Sherwood, I. L. Chuang, *Nature* 414, 883 (2001)
⁸ B. E. Kane, *Nature* 393, 133 (1998)
⁹ D. Deutsch, *Proceedings of the Royal Society A.* 400, 97 (1985)
¹⁰ C. M. Dawson and M. A. Nielsen [arXiv:quant-ph/0505030](https://arxiv.org/abs/quant-ph/0505030).
¹¹ M. Nielsen and I. Chuang, *Quantum Computation and Quantum Information*, Cambridge University Press, 2016, p. 189; ISBN 978-1-107-00217-3.
¹² A. M. Childs, *Phys. Rev. Lett.* 102, 180501 (2009).
¹³ M. Varbanov and T. A. Brun, *Phys. Rev. A* 80, 052330 (2009).
¹⁴ Benjamin A. Blumer, M. S. Underwood, and D. L. Feder, *Phys. Rev. A* 84, 062302 (2011).
¹⁵ A. P. Hines and P. C. E. Stamp, *Phys. Rev. A* 75, 062321 (2007).
¹⁶ N. B. Lovett, S. Cooper, M. Everitt, M. Trevers, V. Kendon, *Phys. Rev. A* 81, 042330 (2010).
¹⁷ A. M. Childs, D. Gosset, Z. Webb, *Science* 339, 791 (2013).
¹⁸ M. S. Underwood and D. L. Feder, *Phys. Rev. A* 82, 042304 (2010).
¹⁹ M. S. Underwood and D. L. Feder, *Phys. Rev. A* 85, 052314 (2012).
²⁰ D. Solenov, *Quantum Information & Computation*, 17, 415 (2017).
²¹ Y. L., Gregory, R. Steinbrecher, A. D. Bookatz and D. Englund, *npj quantum information*, 4, 2 (2018).
²² P. Shor, *Proc. 35th Annual Symp. Foundations of Computer Science* 124 (IEEE, 1994); *SIAM J. Comput.* 26, 1484 (1997).
²³ D. Beckman, A.N. Chari, S. Devabhaktuni, and J. Preskill, *Phys. Rev. A* 54, 1034 (1996)
²⁴ A. Ekert and R. Jozsa, *Rev. Mod. Phys.* 68, 733 (1996).
²⁵ L. M.K. Vandersypen, M. Steffen, G. Breyta, C. S. Yannoni, R. Cleve, I. L. Chuang, *Phys. Rev. Lett. Phys. Rev. Lett.* 85, 25, 5452 (2000)
²⁶ C.-Y. Lu, D. E. Browne, T. Yang and J.-W. Pan, *Phys. Rev. Lett.* 99, 250504 (2007)
²⁷ B. P. Lanyon, T. J. Weinhold, N. K. Langford, M. Barbieri, D. F. V. James, A. Gilchrist, A. G. White, *Phys. Rev. Lett.* 99, 250505 (2007)
²⁸ A. Politi, J. C. F. Matthews, J. L. O'Brien, *Science*, 325, 1221 (2009)
²⁹ E. Martin-Lopez, A. Laing, T. Lawson, R. Alvarez, X.-Q. Zhou, J. L. O'Brien, *Nature Photonics* 6, 773 (2012)
³⁰ E. Lucero, R. Barends, Y. Chen, J. Kelly, M. Mariantoni, A. Megrant, P. O'Malley, D. Sank, A. Vainsencher, J. Wenner, T. White, Y. Yin, A. N. Cleland and J. M. Martinis, *Nature Physics* 8, 719 (2012)
³¹ M. Ezawa, *Phys. Rev. B* 100, 165419 (2019).
³² M. Ezawa, [cond-mat/arXiv:1911.02250v2](https://arxiv.org/abs/cond-mat/1911.02250v2)
³³ F. Buscemi, *Phys. Rev. A*, 83, 012302 (2011)